Toxicon 79 (2014) 64–71

Contents lists available at ScienceDirect

Toxicon

journal homepage: www.elsevier.com/locate/toxicon

Enzyme specificity and effects of gyroxin, a serine protease from the venom of the South American rattlesnake *Crotalus durissus terrificus*, on protease-activated receptors

Camila M. Yonamine [a,*], Marcia Y. Kondo [b], Marcela B. Nering [a], Iuri E. Gouvêa [b], Débora Okamoto [b], Douglas Andrade [b], José Alberto A. da Silva [c], Álvaro R.B. Prieto da Silva [d], Tetsuo Yamane [e], Maria A. Juliano [b], Luiz Juliano [b], Antônio J. Lapa [a,e], Mirian A.F. Hayashi [a], Maria Teresa R. Lima-Landman [a]

[a] *Depto Farmacologia, UNIFESP, São Paulo, SP, Brazil*
[b] *Depto de Biofísica, UNIFESP, São Paulo, SP, Brazil*
[c] *Centro de Biotecnologia-IPEN, São Paulo, SP, Brazil*
[d] *Laboratório de Genética, Instituto Butantan, São Paulo, SP, Brazil*
[e] *Universidade do Estado do Amazonas, Escola Superior de Ciências da Saúde – INCT, Manaus, Amazonas, Brazil*

ARTICLE INFO

Article history:
Received 28 August 2013
Received in revised form 9 December 2013
Accepted 19 December 2013
Available online 8 January 2014

Keywords:
Astrocytes
Barrel rotation syndrome
Gyroxin
Protease-activated receptors
Snake toxin
Serine protease

ABSTRACT

Gyroxin is a serine protease displaying a thrombin-like activity found in the venom of the South American rattlesnake *Crotalus durissus terrificus*. Typically, intravenous injection of purified gyroxin induces a barrel rotation syndrome in mice. The serine protease thrombin activates platelets aggregation by cleaving and releasing a tethered N-terminus peptide from the G-protein-coupled receptors, known as protease-activated receptors (PARs). Gyroxin also presents pro-coagulant activity suggested to be dependent of PARs activation. In the present work, the effects of these serine proteases, namely gyroxin and thrombin, on PARs were comparatively studied by characterizing the hydrolytic specificity and kinetics using PARs-mimetic FRET peptides. We show for the first time that the *short* (*sh*) and *long* (*lg*) peptides mimetizing the PAR-1, -2, -3, and -4 activation sites are all hydrolyzed by gyroxin exclusively after the Arg residues. Thrombin also hydrolyzes PAR-1 and -4 after the Arg residue, but hydrolyzes *sh* and *lg* PAR-3 after the Lys residue. The k_{cat}/K_M values determined for gyroxin using *sh* and *lg* PAR-4 mimetic peptides were at least 2150 and 400 times smaller than those determined for thrombin, respectively. For the *sh* and *lg* PAR-2 mimetic peptides the k_{cat}/K_M values determined for gyroxin were at least 6500 and 2919 times smaller than those determined for trypsin, respectively. The k_{cat}/K_M values for gyroxin using the PAR-1 and -3 mimetic peptides could not be determined due to the extreme low hydrolysis velocity. Moreover, the functional studies of the effects of gyroxin on PARs were conducted in living cells using cultured astrocytes, which express all PARs. Despite the ability to cleavage the PAR-1, -2, -3, and -4 peptides, gyroxin was unable to activate the PARs expressed in astrocytes as determined by evaluating the cytosolic calcium mobilization. On the other hand, we also showed that gyroxin is able to interfere with the activation of PAR-1 by thrombin or by synthetic PAR-1 agonist in cultured astrocytes. Taken together, the data presented here allow us showing that gyroxin cleaves

Abbreviations: PARs, protease-activated receptors; FRET, Fluorescence Resonance Energy Transfer; GPCRs, G-protein-coupled receptors; BBB, blood brain barrier; *sh*, short; *lg*, long; CNS, central nervous system; RSDs, retinal spreading depression waves.

* Corresponding author. Departamento de Farmacologia, Universidade Federal de São Paulo (UNIFESP)/Escola Paulista de Medicina (EPM), Rua 3 de maio 100, Ed. INFAR, 3rd Floor, CEP 04044-020, São Paulo, Brazil. Tel.: +55 11 5576 4447; fax: +55 11 5576 4499.
E-mail address: camilamy@gmail.com (C.M. Yonamine).

0041-0101/$ – see front matter
http://dx.doi.org/10.1016/j.toxicon.2013.12.002

PARs-mimetic peptides slowly and it does not induce activation of PARs in astrocytes. Although gyroxin does not mobilize calcium it was shown to interfere with PARs activation by thrombin and PAR-1 agonist. The determination of gyroxin enzymatic specificity and kinetics on PAR-1, -2, -3, and -4 will potentially help to fill the gap in the knowledge in this field, as the PARs are still believed to have a key role for the gyroxin biological effects.

1. Introduction

Gyroxin is a serine protease that accounts for about 2% of the total protein content of the crude venom of the South American rattlesnake *Crotalus durissus terrificus*. The intravenous injection of this thrombin-like protease into mice triggers the barrel rotation syndrome, which is characterized by rotations of the animal around its long axis (Barrio, 1961). Although the suggestion of a putative intracerebral action of gyroxin involving neurotransmitters release (Cohn and Cohn, 1975), it was shown by others that gyroxin does not affect the release of dopamine and acetylcholine *in vitro* (Camillo et al., 2001).

Several studies exploring different aspects of gyroxin features were reported in the recent years including: (1) the existence of gyroxin structural isoforms, demonstrated by the cloning of five different sequences from a cDNA library of *C. d. terrificus* venom glands (Yonamine et al., 2009); (2) the gyroxin ability to increase blood brain barrier (BBB) permeability (Alves da Silva et al., 2011); (3) the gyroxin action in central nervous system (CNS) suggested by its ability to modify the optical profiles of retinal spreading depression waves (RSDs) in chick retina (Da Silva et al., 2012); and (4) the gyroxin triggered activation of platelet aggregation, potentially mediated by protease-activated receptors (PARs) activation (Da Silva et al., 2012), suggested based on the thrombin mechanism of action that requires PARs to trigger the platelet aggregation (Coughlin, 1999; Kahn et al., 1998).

PARs are members of seven-transmembrane G-protein-coupled receptors (GPCRs) family, whose activation is triggered by the cleavage of specific sites at the N-terminus of receptor by serine proteases, resulting in the generation of a tethered ligand that interacts with the receptor within its extracellular loop-2 (Macfarlane et al., 2001). The binding of this ligand to the core of PARs initiates an intracellular signal transduction pathway, which involves both phosphoinositide breakdown and cytosolic calcium mobilization (Macfarlane et al., 2001).

The mechanism of activation of PARs (-1, -2, -3, and -4) by serine proteases followed by the intracellular signaling pathways, and their consequent physiological and pathophysiological roles are well studied (Macfarlane et al., 2001). Rat astrocytes express PAR-1, -2, -3, and -4, but the calcium signal evoked by PAR-3 and -4 agonist peptides is relatively weaker compared to that induced by PAR-1 or -2 agonists (Wang et al., 2002).

Activation of human platelets by thrombin involves the proteolytic activation of PAR-1 and PAR-4 (Coughlin, 1999; Kahn et al., 1998). Low concentrations of thrombin is enough to activate PAR-1 in human platelets, due to its high-affinity, while PAR-4 is a low-affinity receptor, requiring higher concentrations of thrombin for signaling activation (Mao et al., 2008).

Gyroxin also promotes platelet aggregation and the involvement of PARs was suggested (Da Silva et al., 2012). In fact, a significant inhibition of platelet aggregation induced by gyroxin was observed in the presence of antagonists of PAR-1 [SCH79797] or PAR-4 [tcY-NH2]. Interestingly, PAR-1 antagonist inhibits platelet aggregation triggered by gyroxin at concentrations of about two orders of magnitude smaller than that required for PAR-4 antagonist, and the combination of these two antagonists determined only a partial inhibition of the platelet aggregation induced by gyroxin (Da Silva et al., 2012).

Up to now, despite the several similar enzymatic features shared by both serine proteases, *e.g.* gyroxin and thrombin, the potential effects of gyroxin on PARs are still poorly described. So forth, the characterization of the enzymatic specificity of gyroxin on PAR-1, -2, -3, and -4, and the evaluation of the PARs activation by gyroxin in living cells, monitored by the free intracellular calcium concentration ($[Ca^{2+}]i$) increases might help to fill the gap in the knowledge in this field.

2. Material and methods

Ethics statement: The protocol was approved by the Committee on the Ethics of Animal Experiments of Universidade Federal de Sao Paulo (UNIFESP) (CEP Number: 2003/09).

2.1. Purification of gyroxin

Crotamine negative venom of *C. d. terrificus* was kindly provided by Dr. Eduardo B. Oliveira (Departamento de Bioquímica e Imunologia, Universidade de São Paulo, Ribeirão Preto, Brazil). Gyroxin was obtained by fractionating the crude venom by employing affinity chromatography and molecular exclusion as previously described (Alves da Silva et al., 2011). As gyroxin is a serine protease, the use of organic solvent was consistently avoided to assure that the enzymatic activity properties were not lost in the purification steps. The collected fractions containing purified gyroxin were combined in a conical tube, and the protein concentration was determined by Bradford method (Bradford, 1976). The samples were cooled, lyophilized and stored at −20 °C.

2.2. Neurotoxicity assay

To confirm that the biological activity of gyroxin was not lost during the purification process, a neurotoxicity assay that allows observing the barrel rotation syndrome

characteristic of the pure gyroxin (Barrio, 1961) was performed. Five Swiss mice (males) weighing 25–35 g were injected with 0.5 mg/kg of purified gyroxin dissolved in 150 mM NaCl by intravenous (i.v.) route. After injection, each animal was monitored for up to 60 min to observe the barrel rotation activity.

2.3. Gel electrophoresis and western blotting analysis

The purified gyroxin, as described above from the rattlesnake venom, was then resolved by denaturing 12.5% polyacrylamide gel electrophoresis (SDS-PAGE) (Laemmli, 1970) and analyzed by Western blotting (WB). The gels with the separated proteins [0.01 or 5 μg of gyroxin] were either transferred to nitrocellulose membrane for WB or stained with Coomassie brilliant blue R-250, respectively. The WB membrane was blocked 1 h with 3% bovine serum albumin (BSA) before the overnight incubation, at room temperature, with the horse anti-crotalic serum provided by Butantan Institute (diluted 1:1000 in TBST [500 mM Tris–HCl pH 8.0, 0.9% NaCl w/v, 0.05% Tween-20, v/v]). The recognized immune-complexes were detected using a secondary antibody anti-horse conjugated to horseradish peroxidase [1:5000 in TBST], after addition of *ECL Plus western blotting detection system* (GE Healthcare, Buckinghamshire, UK). The protein markers used were Unstained Protein Molecular Weight Marker (Fermentas, Maryland, USA) and ECL DualVue western blotting markers (GE Healthcare).

2.4. MALDI-TOF-mass spectrometry

Aliquots of gyroxin [30 μM] were mixed with 20 μL of matrix solution (0.5 mol/L 2,5-dihydroxybenzoic acid solution in methanol containing 0.1% trifluoroacetic acid) (Schiller et al., 1999). Subsequently, samples were brought onto the sample plate and dried at room temperature, before the analysis using a matrix-assisted laser desorption/ionization time of flight (MALDI-TOF) Microflex LT model (Bruker Daltonics Inc., Billerica, USA).

2.5. Peptide synthesis

All quenched fluorescent substrates, based on Fluorescence Resonance Energy Transfer (FRET) technology were obtained by solid-phase peptide synthesis strategy as previously described (Hirata et al., 1995). The peptides derived sequences that span the cleavage sites for human PAR-1, -2, -3, and -4 activation were based on previous work (Coughlin, 1999), and they were synthesized with the fluorescent and quenching group at the N- and C-terminus end, respectively. Stock solutions of peptides were prepared in dimethyl sulfoxide (DMSO), and the final concentration was determined spectrophotometrically using the molar extinction coefficient of 17,300 M^{-1} cm^{-1} at 365 nm.

2.6. Enzymatic assays

Hydrolysis of FRET peptides was quantified using a spectrofluorimeter F-2500 model (Hitachi, Tokyo, Japan), which allow the measurements of the excitation fluorescence at 320 nm and emission at 420 nm (Melo et al., 2001).

The scissile bond of hydrolyzed peptides were identified by isolation of the fragments using analytical high-performance liquid chromatography (HPLC) followed by the determination of these peptide fragments molecular mass by liquid chromatography–mass spectrometry (LC/MS) using an LCMS-2010 equipped with an ESI-probe (Shimadzu, Kyoto, Japan).

2.7. Kinetic parameters determination

The assays were performed in HBSS (Hank's Buffered Salt Solution) buffer [1.3 mM CaCl2, 0.5 mM $MgCl_2 \cdot 6H_2O$, 0.4 mM $MgSO_4 \cdot 7H_2O$, 5.3 mM KCl, 0.4 mM KH_2PO_4, 140 mM NaCl, 0.34 mM $NaH_2PO_4 \cdot 7H_2O$, 5.5 mM D-glucose, 20 mM HEPES (4-(2-hydroxyethyl)-1-piperazineethanesulfonic acid) pH 7.4] at 37 °C. HBSS buffer was used in this experiment to assure the same assay conditions used for measuring the free cytosolic calcium concentration $[Ca^{2+}]i$ in cultured astrocyte cells.

The hydrolysis kinetic parameters (k_{cat}, K_M, and k_{cat}/K_M) of gyroxin and thrombin were determined based on initial rate measurements at 8–10 s, with substrate concentrations between 0.5 and 30 mM. The enzyme concentration [0.3 μM] chosen were such that less than 5% of the substrate was hydrolyzed over the course of the assay. The reaction rate was converted into micromoles of substrate hydrolyzed per min, based on a calibration curve obtained after a complete hydrolysis of each peptide. The data was fitted to the Michaelis–Menten equation using Grafit software (Erithacus Software, Horley, Surrey, UK), with the corresponding standard errors values. For all assays, data were collected and the error values were less than 10% for each of the obtained kinetic parameter. The data were expressed as mean ± SE, $N = 3$.

2.8. Determination of the substrate cleavage sites

After the hydrolyzes assays, 20 μM of each substrate was incubated at 37 °C overnight and the scissile bonds of hydrolyzed FRET peptides were identified by isolation of the fragments using analytical HPLC, followed by the amino acid analysis and molecular mass determinations by a LC/MS analysis using a LCMS-2010EV model, equipped with an ESI-probe (Shimadzu, Kyoto, Japan).

2.9. Primary culture of astrocytes

Primary astrocyte-enriched cell cultures were obtained from eight newborn rats (Hamprecht and Löffler, 1985). In brief, the newborn rats were sacrificed by decapitation, and the brains were collected in HBSS buffer. Cerebral cortex was dissected and the cells were dissociated by trituration using a Pasteur pipette. After filtration (100 μm), the cells were cultured in Dulbecco's modified Eagle's medium (DMEM) (Invitrogen, Carlsbad, CA, USA) containing 10% heat-inactivated fetal bovine serum (FBS) (Invitrogen), 100 U/mL penicillin, and 100 μg/mL streptomycin (Invitrogen) at 37 °C, in a humidified incubator with 5% CO_2. The medium was changed for the first time in the next day and,

thereafter, at every 2–3 days, depending on the cell density. For the experiments conducted here, the cells cultured from day 7–14 were used.

2.10. Cytotoxicity assay

The cytotoxicity effects of gyroxin and thrombin were evaluated using the tetrazolium (XTT) (Sigma–Aldrich, St. Louis, USA) assay (Goodwin et al., 1995), with minor modifications. Bioreduction of XTT usually requires addition of an intermediate electron acceptor, phenazine methosulphate (PMS), prepared and stored in the dark at −20 °C, until required. The primary astrocyte cells, from 7 to 10 days of culture, were plated in a 96-wells microplate [10,000 cells/well] that was incubated in humidified 5% CO_2 air incubator, for 24 h. The thrombin used in this work (Lot No. 091 M 700 7V, Sigma–Aldrich, St. Louis, USA), 2777 U correspond to 1 mg of protein.

Gyroxin [0.3, 3, 30, and 300 nM] and thrombin [0.01, 0.1, 1, and 10 nM] were dissolved in DMEM medium without phenol red (Sigma–Aldrich) containing 10% FBS, 100 U/mL penicillin, and 100 μg/mL streptomycin. Then, 100 μL of this mixture were added to each well before the incubation in a humidified 5% CO_2 air incubator for further 24 h. Phenol solution [0.04, 0.08, 0.15, and 0.30%] was used as positive control of cell death, due to its well-known high cytotoxic activity (Fabre et al., 2001).

Then, 10 μL of PMS [1.53 mg/mL] was added to 1 mL of XTT solution [1 mg/mL in PBS buffer], immediately before use. After warming up to 37 °C, 50 μL of this solution was added to each well of the microplate containing the treated cells. The plates were then incubated in the humidified 5% CO_2 air incubator for 3 h, and the OD_{490nm} were determined in a microplate reader (Spectramax M5, Molecular Devices LLC., Sunnyvale, CA, USA). The obtained data were statistically analyzed by Oneway-ANOVA, Dunnett's Multiple Comparison Test ($p < 0.05$), and expressed as mean ± SEM of three independent experiments.

2.11. Cytosolic free calcium measurements

The intracellular free calcium concentration ($[Ca^{2+}]_i$) was determined using the free calcium sensitive fluorescent dye Fura-4 (FLIPR Calcium 4 Assay kit, Molecular Devices).

The primary astrocyte cells culture, from 7 to 10 days of culture, were plated in 96-wells plate reader [20,000 cells/well] in DMEM medium with 10% FBS, without antibiotics, and the cells were incubated in the humidified 5% CO_2 air incubator for 24 h. The cells were then loaded for 1 h at 37 °C with 5 μM Fluo-4-AM containing 2.5 mM of probenecid in HBSS buffer, before the stimulation with the following agonists: 0.3 μM of gyroxin, 0.1 nM of thrombin, 1 μM of PAR-1 agonist (SFLLRN-NH2), and PAR-4 agonist (AYPGKF-NH2) [1, 10, or 100 nM]. Cell responsiveness was assured by measuring the cell response to 70 mM KCl.

The PAR-1 antagonist (SCH79797) (Tocris Bioscience, Minneapolis, USA) [3,10, 35, 70, and 140 nM] was added to the cultured cells medium 30 min before the addition of the 0.1 nM of thrombin, and 35 nM PAR-1 antagonist was added 30 min before addition of 1 μM of PAR-1 agonist.

In order to verify the potential effect of gyroxin on the PAR-1 activation by 0.1 nM of thrombin or 1 μM of PAR-1 agonist, this toxin [0.3 μM] was added 1.5 h before the assay. Calcium responses were measured using excitation at 470–495 nm and emission at 515–575 nm in a FlexStation microplate reader (Molecular Devices) (Sun et al., 2010). Responses to agonist addition were determined as peak fluorescence minus the basal fluorescence intensity using the SoftMax®Pro software (Molecular Devices Corp.). The obtained data were statistically analyzed by One-Way ANOVA, Bonferroni's multiple comparison test ($p < 0.05$), and are presented as mean ± SEM of 3 experiments.

3. Results

3.1. Gyroxin purification and biological activity confirmation

A single band of about 30 kDa was observed in both SDS-PAGE and Western blotting analysis of the gyroxin purified here from the crude venom. Moreover, MALDI-TOF MS analysis of this purified material also confirmed a single molecular weight of about 29,370 kDa for this sample (data not shown).

Aiming to confirm that the purified gyroxin obtained here was biologically active, this purified gyroxin (0.5 mg/kg) was administered by a single intravenous (i.v.) injection in mice ($n = 6$), which allowed to observe alterations in motor behavior and the typical barrel rotation syndrome, as previously described by others (Barrio, 1961; Alexander et al., 1988; Alves da Silva et al., 2011). The barrel rotation phenotype started from 3 to 5 min after gyroxin injection, and this process remained for approximately 2 min. In our hands, the animals in general returned to their normal behavior 1 h after the gyroxin injection (data not shown).

3.2. Kinetic parameters determination

Since proteases usually require a broader surface of contact with their substrate for the cleavage site recognition (Li et al., 2010), herein we have designed and used two versions of the substrate peptides mimetizing the cleavage site, namely short (*sh*) and long (*lg*) peptides, which consisted of 10 and 20 amino acid residues long sequences, respectively. In this work, both the *sh* and *lg* mimetic peptides for all PARs were analyzed in order to verify if the *lg* version of the PARs mimetic peptides could also be hydrolyzed at other potential N-terminal cleavage sites of these peptides as described for the *sh* and *lg* PAR-2 mimetic peptides (Al-Ani and Hollenberg, 2003).

The *sh* PAR-2 is hydrolyzed by gyroxin at SSKGR↓SLIG, in the same way as trypsin (Macfarlane et al., 2001), while the *lg* PAR-2 is hydrolyzed at three different sites, namely QGTNR↓SSKGR↓SLIGR↓VDGT, representing 2, 42, and 56% of the cleavage, respectively, as determined by HPLC (Table 1). Moreover, the k_{cat}/K_M values for gyroxin were found to be about 6500 and 2919 times smaller than that determined for trypsin for *sh* and *lg* PAR-2, respectively (Table 1).

The gyroxin and thrombin cleavage specificity of *sh* and *lg* PARs-1, -3, and -4 peptides, as well as the respective kinetics parameters determined for each peptide substrates, are listed in Table 2. Gyroxin hydrolyzes both *sh* and *lg* PAR-

Table 1
Values of k_{cat}, K_M and k_{cat}/K_M for thrombin and gyroxin using FRET peptides mimetizing the sequences that span the cleavage sites of human PAR-2.

Peptide	Trypsin	Trypsin			Gyroxin	Gyroxin		
	Sequence Abz-peptidyl-EDDnp	k_{cat} (s^{-1})	K_M (μM)	k_{cat}/K_M $(mM\ s)^{-1}$	Sequence Abz-peptidyl-EDDnp	k_{cat} (s^{-1})	K_M (μM)	k_{cat}/K_M $(mM\ s)^{-1}$
PAR-2 short	SSKGR↓SLIG	8.9 ± 0.8	7.7 ± 1.1	1170	SSKGR↓SLIG	0.002 ± 0.00015	10.8 ± 3.4	0.18
PAR-2 long	QGTNRSSKGR↓SLIGRVDGT	6.1 ± 0.9	4.1 ± 1.4	1255	QGTNR↓SSKGR↓SLIGR↓VDGT	0.008 ± 0.00300	19.0 ± 2.0	0.43

Gyroxin and trypsin hydrolyzes the peptides PAR-2 (*sh*/*lg*) after Arg (R) residues. The cleavage sites are indicated by arrows (↓). The data are presented as mean ± SE ($N = 3$). PAR-2 (*lg*) was hydrolyzed by gyroxin at QGTNR↓SSKGR↓SLIGR↓VDGT, showing 2%, 42%, and 56% of cleavage, respectively.

1 and -4 peptides at R↓S and R↓G, respectively, showing the same specificity determined for thrombin (Table 2). Both *sh* and *lg* PAR-3 peptides are hydrolyzed by gyroxin after Arg residue (Table 2), while thrombin cleaves PAR-3 peptide after the Lys residue, as also described by Macfarlane et al. (2001).

Even when the cleavage specificity was shown to be the same for both *sh* and *lg* versions of the PARs-mimetic peptides, differences in the kinetic parameters were observed. For instance, the k_{cat}/K_M values for gyroxin determined with the *sh* and *lg* PAR-4 peptides were 2150 and 400 times smaller than that determined for thrombin, respectively, showing a more prominent difference among gyroxin and thrombin with the *sh* peptides (Table 2). In the same way, the k_{cat}/K_M values determined for gyroxin with the *sh* and *lg* PAR-2 peptides were about 6500 and 2919 times, respectively, smaller than those determined for trypsin (Table 1).

Unfortunately, the kinetics parameters for gyroxin hydrolysis with *sh* and *lg* versions of PAR-1 and PAR-3 peptides, and also for thrombin hydrolysis of *sh* and *lg* PAR-3 peptides, could not be determined due to the low hydrolysis velocity of these peptides (Table 2).

3.3. Cytotoxicity assay and cytosolic free calcium measurements

The XTT assay performed for thrombin [0.01, 0.1, 1, and 10 nM] and gyroxin [0.3, 3, 30, and 300 nM] did not allow observing significant toxic effects for astrocytes after 24 h incubations (data not shown). Taking this into account, the effects of gyroxin on PARs were assessed in cultured astrocyte at a concentration of 300 nM.

The reliance upon cytosolic free calcium measurements was guaranteed by using thrombin, which showed an effective action as agonist of PAR-1 (Coughlin, 2000), as a positive control. In fact, thrombin evoked increases of $[Ca^{2+}]_i$ that was blocked by PAR-1 antagonist (SCH79797) in a concentration-dependent manner (Fig. 1A). Accordingly, in our hands, both thrombin [0.1 nM] and also PAR-1 agonist SFLLRN [1 μM] triggered $[Ca^{2+}]_i$ responses in cultured rat astrocytes, and this increase was blocked by 35 nM PAR-1 antagonist (Fig. 1B). At the employed concentrations, gyroxin [300 nM] and PAR-4 agonist AYPGKF-NH_2 [1, 10, and 100 μM] were unable to trigger a significant increase in $[Ca^{2+}]_i$ in this same astrocytes primary culture (Fig. 1C).

The inability of gyroxin to activate PAR-1 in cultured astrocytes (Fig. 1C and D) is consistent with the fact that gyroxin cleaves *sh* and *lg* PAR-1 peptides very slowly, *i.e.* the hydrolysis of these peptides by gyroxin could be observed only after overnight incubation, which hampered the determination of the kinetic parameters for gyroxin using these peptides (Table 2). On the other hand, gyroxin was consistently able to antagonize the activation of PAR-1 receptor by both thrombin and PAR-1 agonist (Fig. 1D).

4. Discussion

The goal of the present study is to better understand the effects of gyroxin on protease-activated receptors (PARs), aiming to explore their potential involvement in the biological features described for gyorxin (Barrio, 1961; Alexander et al., 1988; Alves da Silva et al., 2011). Gyroxin is a thrombin-like enzyme (Alexander et al., 1988) and the PARs are activated by the cleavage of its N-terminus by

Table 2
k_{cat}, K_M and k_{cat}/K_M values for hydrolysis by thrombin and gyroxin of the FRET peptides derived sequences that span the cleavage sites for human PAR-1, -3 and -4.

Peptide	Sequence Abz-peptidyl-EDDnp	Thrombin			Gyroxin		
		k_{cat} (s^{-1})	K_M (μM)	k_{cat}/K_M $(mM\ s)^{-1}$	k_{cat} (s^{-1})	K_M (μM)	k_{cat}/K_M $(mM\ s)^{-1}$
PAR-1 short	TLDPR↓SFLLQ	10.0 ± 0.6	21 ± 2.7	500	ND	ND	ND
PAR-1 long	KATNATLDPR↓SFLLRNPNDQ	8.0 ± 0.3	20 ± 1.5	400	ND	ND	ND
PAR-4 short	LPAPR↓GYPGQ	28.5 ± 2.0	33 ± 3.4	860	0.012 ± 0.0008	27 ± 3.0	0.40
PAR-4 long	STPSILPAPR↓GYPGQVCANQ	6.6 ± 0.4	31 ± 3.3	200	0.010 ± 0.0003	21 ± 1.5	0.50

Gyroxin hydrolyzes the peptides PAR-1 and -4 (*sh*/*lg*) at R↓S and at R↓G at the same cleavage sites described for thrombin. The cleavage sites are indicated by the arrows (↓). ND means that the velocity of cleavage was so low that it was not possible to determine the kinetic parameters. The data are presented as mean ± SE ($N = 3$).
PAR-3 peptides (*sh*/*lg*) were hydrolyzed by gyroxin after Arg (R) residues: Abz- TLPIKTFR↓GQ-EDDnp and Abz- NLAKPTLPIKTFR↓GAPPNSQ-EDDnp. Thrombin hydrolyzed after Lys (K) residues: Abz-TLPIK↓TFRGQ-EDDnp and Abz- NLAKPTLPIK↓TFRGAPPNSQ-EDDnp. The kinetics parameters of PAR-3 peptides (*sh*/*lg*) could not be determined for both gyroxin and thrombin.

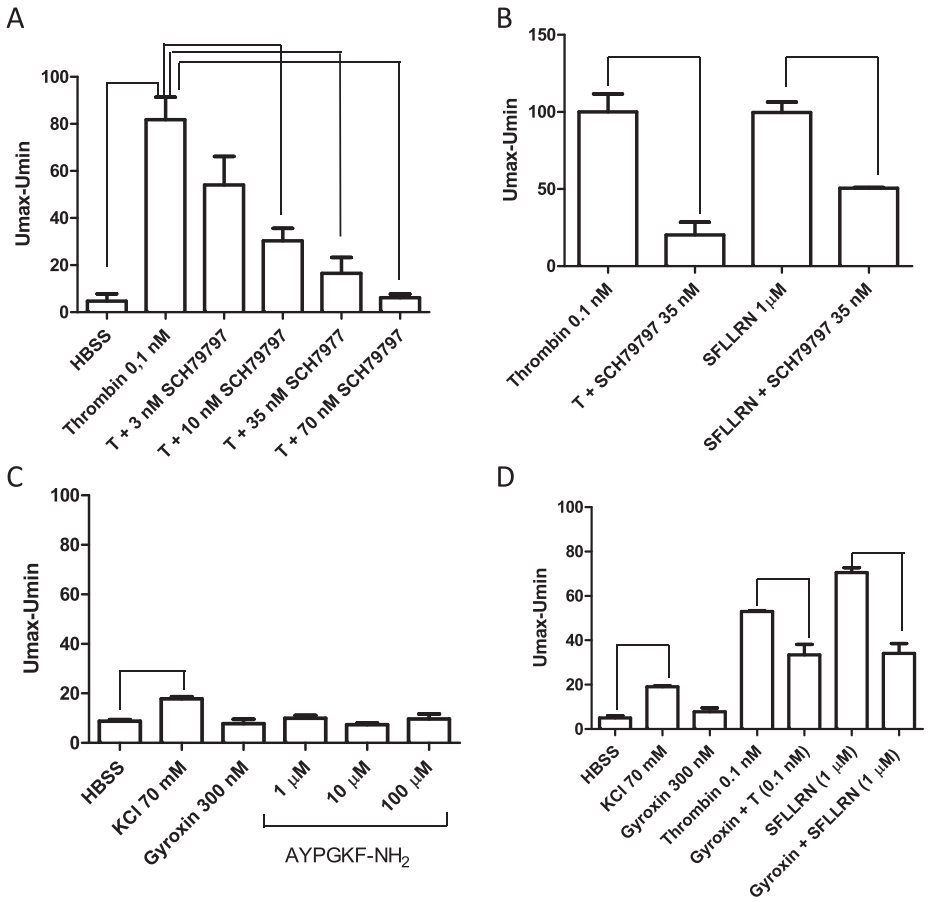

Fig. 1. Calcium released by thrombin and PAR-1-agonist in astrocytes culture and inhibition by gyroxin and PAR-1-antagonist. The graphics show the peak fluorescence (U_{max}) minus the basal fluorescence (U_{min}) intensity value in response to the agonist addition ($U_{max} - U_{min}$): (A) Astrocyte cells stimulated with thrombin [0.1 nM], in the absence or presence of PAR-1 antagonist (SCH79797) [3, 10, 35, and 70 nM], which were added 30 min before the assay; (B) Astrocyte cells stimulated with 0.1 nM of thrombin or 1 μM of PAR-1 agonist (SFLLRN-NH2), in the absence or presence of 35 nM of PAR-1 antagonist SCH79797, added 30 min before the assay; (C) Astrocyte cells stimulated with 70 mM of KCl, gyroxin [0.3 μM] or PAR-4 agonist (AYPGKF-NH2) [1, 10, and 100 μM]; (D) Astrocyte cells stimulated with 0.1 nM of thrombin, 1 μM of PAR-1 agonist, 70 mM of KCl or 0.3 μM of gyroxin, and for the stimulation with 0.1 nM of thrombin or 1 μM of PAR-1 agonist, gyroxin was pre-incubated for 1.5 h with the cells before the assay. The obtained data were statistically analyzed by One-Way ANOVA Bonferroni's Multiple Comparison Test of 3 independent experiments, and are presented as mean ± SEM. Comparisons with $^{*}p < 0.05$ are indicated by the bars. U_{max} corresponds to the final arbitrary fluorescence value of free Ca^{2+} measured with Fura-4 fluorescent dye after the addition of agonist, and U_{min} corresponds to baseline of fluorescence value. 1 U/mL of thrombin corresponds to 9.7 nM.

serine proteases as thrombin, leading to suggest the involvement of PARs in the biological functions of gyroxin (Da Silva et al., 2012) Moreover, biodistribution studies for labeled ^{125}I-gyroxin showed a tissue distribution that correlates with the expression of PARs (Alves da Silva et al., 2006). Herein the effects of gyroxin on PARs were consistently studied by using biochemical (enzyme kinetics) and cellular assays.

Gyroxin hydrolyzed both *sh* and *lg* versions of PAR-1 and PAR-4 peptides at the same cleavage sites also described for thrombin (Kahn et al., 1998). However, gyroxin does not cleave the *lg* PAR-1 peptide after the second Arg (R) located close to the Asp (N) residue (Table 2). This is most likely due to the large size of the Asp (N) residue side chain, as bulk side chains and changes in the rigidity or geometry of binding sites are the main factors that affect enzyme–substrate interactions and the subsequent catalytic process (Okamoto et al., 2010). PAR-3 peptides (*sh*/*lg*) were hydrolyzed by gyroxin after Arg residue (Table 2), while thrombin cleaves PAR-3 peptide after the Lys residue (Macfarlane et al., 2001).

In our hands, trypsin cleaved PAR-2 peptides (*sh*/*lg*) in one single position (Table 1), similarly as described by Al-Ani and Hollenberg (2003), while PAR-2 peptides (*sh*/*lg*) were hydrolyzed by gyroxin after all Arg residues, which in accordance to our previous work (Yonamine et al., 2012).

The involvement of PARs activation in the platelet aggregation triggered by gyroxin was suggested by Da Silva et al. (2012), as the antagonists of PAR-1 [SCH79797] and PAR-4 [tcY-NH2] promoted a significant inhibition of platelet aggregation induced by gyroxin. The antagonist of PAR-1 was about two orders of magnitude more effective than the PAR-4 antagonist, and the combination of these two antagonists did not completely inhibit the platelet

aggregation triggered by gyroxin (Da Silva et al., 2012). However, we show here that gyroxin cleaves PARs peptides very slowly. Therefore, it is hard to believe that the effects observed for gyroxin on platelet aggregation could be associated with PARs cleavage and consequent activation, in spite of the demonstration of the gyroxin-induced platelet aggregation inhibition by the PAR-1 and PAR-4 antagonists (Da Silva et al., 2012).

Cultured astrocytes constitutively express PAR-1, -2, -3, and -4 (Wang et al., 2002). Thrombin evokes increases of $[Ca^{2+}]_i$ in astrocyte cells with an EC_{50} value of about 1×10^{-2} U/mL (Ubl and Reiser, 1997) and, so forth, it was used as a positive control for the reliance upon cytosolic $[Ca^{2+}]_i$ measurements in astrocyte cells.

In our hands, increased $[Ca^{2+}]i$ induced by thrombin [0.1 nM] could be blocked by PAR-1 antagonist in a concentration-dependent manner (Fig. 1A and B), similarly as previously described by others (Kahn et al., 1998; Ubl and Reiser, 1997).

We also show in this work that the thrombin and PAR-1 agonist induced $[Ca^{2+}]_i$ increases were effectively blocked by gyroxin (Fig. 1D), possibly suggesting that gyroxin may bind to PAR-1 receptor to interfere with its activation by thrombin and PAR-1 agonist. The enzymatic action of gyroxin in other sites of PAR-1 cannot be ruled out at the moment, but the calcium signal evoked in astrocytes by gyroxin was too weak to justify any further studies on the gyroxin enzymatic and binding specificity on this receptor, except if it is underlying the blockage of the thrombin and PAR-1 agonist effects (Fig. 1D).

There is very strong evidence that PAR-1 plays a protective role in maintaining endothelial barrier integrity. The global inhibition of PAR-1 may disrupt the endothelial barrier protective signals and present as an increase in bleeding (Ramachandran, 2012). Gyroxin is able to increase the blood–brain barrier permeability (Alves da Silva et al., 2011) and the blockage of PAR-1 by gyroxin could be potentially related to the mechanism of action responsible for this effect. However, we are aware that further studies specifically conducted to demonstrate the direct interaction of gyroxin with the PAR-1, and the respective mechanism(s) of action underlying this effect are still necessary.

On the other hand, PAR-4 agonist peptides evoked a calcium signal relatively weaker than that induced by PAR-1 in astrocytes (Fig. 1C), as also described by Nakanishi-Matsui et al. (2000). Thereby the gyroxin effects on PAR-4 receptor using this specific biological assay and under the conditions employed by us could not be evaluated here. Indeed, the calcium signal evoked by PAR-3 and -4 agonist peptides in rat astrocytes is relatively weaker compared to that induced by PAR-1 or -2 agonists (Wang et al., 2002).

Taken together, considering the irrelevant ability of gyroxin to cleave PARs peptides at the activation cleavage site and to trigger cell signaling through calcium mobilization in astrocytes, we suggest here that gyroxin might not be able to activate PARs. Nevertheless the direct involvement of PARs in gyroxin biological effects, including the platelet activation, cannot be completely ruled out, as gyroxin is able to interfere in the thrombin and PAR-1 agonist effects.

5. Conclusion

In this work, the cleavage specificity of gyroxin on PAR-1, -2, -3, and -4 mimetic peptides substrates was determined for the first time. However gyroxin was unable to activate PARs expressed in astrocytes as determined here by evaluating the cytosolic calcium mobilization. On the other hand, a putative effect of gyroxin as a potential PAR-1 antagonist, acting by blocking the activation of PAR-1 receptor by thrombin or by its specific agonist (SFLLRN-NH2) was demonstrated here. These results suggest that the direct activation of PARs by gyroxin is unlikely, although the PARs involvement in the biological effects of gyroxin, including the platelet activation, cannot be completely ruled out. As the nadir of the field is the biochemical and enzymatic specificity characterization of gyroxin, we believe that this work will potentially help to fill the gap in the knowledge in this field, regarding the PARs roles for the gyroxin biological effects.

Acknowledgment

the authors acknowledge CAPES, CNPq, and FAPESP for the financial support. We are also grateful to Dr. Eduardo Brandt Oliveira (Departamento de Bioquímica e Imunologia, Universidade de São Paulo, Ribeirão Preto) for the kind supply of *C. d. terrificus* venom, and to Dr. João E. Oliveira and Dr. Maria Aparecida Camillo (Centro de Biotecnologia-IPEN) for the support on gyroxin purification, and Dr. Vitor Oliveira (Departamento de Biofísica - UNIFESP/EPM) for the fruitful discussions.

Conflict of interest

The authors have no conflict of interest to declare.

References

Al-Ani, B., Hollenberg, M.D., 2003. Selective tryptic cleavage at the tethered ligand site of the amino terminal domain of proteinase-activated receptor-2 in intact cells. J. Pharmacol. Exp. Ther. 304, 1120–1128.

Alexander, G., Grothusen, J., Zepeda, H., Schwartzman, R.J., 1988. Gyroxin, a toxin from the venom of *Crotalus durissus terrificus*, is a thrombin-like enzyme. Toxicon 26, 953–960.

Alves da Silva, J.A.A., Muramoto, E., Ribela, M.T.C.P., Rogero, J.R., Camillo, M.A.P., 2006. Biodistribution of gyroxin using 125I as radiotracer. J. Radioanal. Nucl. Chem. 269, 579–583.

Alves da Silva, J.A., Oliveira, K.C., Camillo, M.A.P., 2011. Gyroxin increases blood-brain barrier permeability to Evans blue dye in mice. Toxicon 57, 162–167.

Barrio, A., 1961. Gyroxin, a new neurotoxin of *Crotalus durissus terrificus* venom. Acta Physiol. Latinoam. 11, 224–232.

Bradford, M.M., 1976. A rapid and sensitive method for the quantitation of microgram quantities of protein utilizing the principle of protein-dye binding. Anal. Biochem 72, 248–254.

Camillo, M.A.P., Arruda-Paes, P.C., Troncone, L.R.P., Rogero, J.R., 2001. Gyroxin fails to modify in vitro release of labelled dopamine and acetylcholine from rat and mouse striatal tissue. Toxicon 39, 843–853.

Cohn, M.I., Cohn, M., 1975. Barrel rotation induced by somatostatin in the non-lesioned rat. Brain Res. 96, 138–141.

Coughlin, S.R., 1999. How the protease thrombin talks to cells. Proc. Natl. Acad. Sci. U. S. A. 96, 11023–11027.

Coughlin, S.R., 2000. Thrombin signalling and protease-activated receptors. Nature 407, 258–264.

Da Silva, J.A.A., Spencer, P., Camillo, M.A.P., De Lima, V.M.F., 2012. Gyroxin and its biological activity: effects on CNS basement membranes and endothelium and protease-activated receptors. Curr. Med. Chem. 19, 281–291.

Fabre, T., Schappacher, M., Bareille, R., Dupuy, B., Soum, A., Bertrand-Barat, J., Baquey, C., 2001. Study of a (trimethylenecarbonate-co-epsiloncaprolactone) polymer–part 2: in vitro cytocompatibility analysis and in vivo ED1 cell response of a new nerve guide. Biomaterials 22, 2951–2958.

Goodwin, C.J., Holt, S.J., Downes, S., Marshall, N.J., 1995. Microculture tetrazolium assays: a comparison between two new tetrazolium salts, XTT and MTS. J. Immunol. Methods 179, 95–103.

Hamprecht, B., Löffler, F., 1985. Primary glial cultures as a model for studying hormone action. Methods Enzymol. 109, 341–345.

Hirata, I.Y., Cezari, M.H.S., Nakaie, C.R., Boschcov, P., Ito, A.S., Juliano, M.A.P., Juliano, L., 1995. Internally quenched fluorogenic protease substrates: solidphase synthesis and fluorescence spectroscopy of peptides containing orthoaminobenzoyl/dinitrophenyl groups as donor-acceptor pairs. Lett. Pept. Sci. 6, 299–308.

Kahn, M.L., Zheng, Y.W., Huang, W., Bigornia, V., Zeng, D., Moff, S., Farese Jr., R.V., Tam, C., Coughlin, S.R., 1998. A dual thrombin receptor system for platelet activation. Nature 394, 690–694.

Laemmli, U.K., 1970. Cleavage of structural proteins during the assembly of the head of bacteriophage T4. Nat. Lond. 227, 680–685.

Li, M., Chen, C., Davies, D.R., Chiu, T.K., 2010. Induced-fit mechanism for prolyl endopeptidase. J. Biol. Chem. 285 (28), 21487–21495.

Macfarlane, S.R., Seatter, M.J., Kanke, T., Hunter, G.D., Plevin, R., 2001. Proteinase activated receptors. Pharmacol. Rev. 53, 245–282.

Mao, Y., Jin, J., Kunapuli, S.P., 2008. Characterization of a new peptide agonist of the protease-activated receptor-1. Biochem. Pharmacol. 75, 438–447.

Melo, R.L., Alves, L.C., Del Nery, E., Juliano, L., Juliano, M.A., 2001. Synthesis and hydrolysis by cysteine and serine proteases of short internally quenched fluorogenic peptides. Anal. Biochem 293, 71–77.

Nakanishi-Matsui, M., Zheng, Y.W., Sulciner, D.J., Weiss, E.J., Ludeman, M.J., Coughlin, S.R., 2000. PAR3 is a cofactor for PAR4 activation by thrombin. Nature 404, 609–613.

Okamoto, D.N., Kondo, M.Y., Hiraga, K., Juliano, M.A., Juliano, L., Gouvea, I.E., Oda, K., 2010. Salt effect on substrate specificity of a subtilisin-like halophilic protease. Protein Pept. Lett. 17, 796–802.

Ramachandran, R., 2012. Developing PAR1 antagonists: minding the endothelial gap. Discov. Med. 13 (73), 425–431.

Schiller, J., Arnhold, J., Benard, S., Müller, M., Reichl, S., Arnold, K., 1999. Lipid analysis by matrix-assisted laser desorption and ionization mass spectrometry: a methodological approach. Anal. Biochem 267, 46–56.

Sun, Z.W., Zhang, L., Zhu, S.J., Chen, W.C., Mei, B., 2010. Excitotoxicity effects of glutamate on human neuroblastoma SH-SY5Y cells via oxidative damage. Neurosci. Bull. 26, 8–16.

Ubl, J., Reiser, G., 1997. Characteristics of thrombin-induced calcium signals in rat astrocytes. Glia 21, 361–369.

Wang, H., Ubl, J.J., Reiser, G., 2002. Four subtypes of protease-activated receptors, co-expressed in rat astrocytes, evoke different physiological signaling. Glia 37, 53–63.

Yonamine, C.M., Kondo, M.Y., Juliano, M.A., Icimoto, M.Y., Rádis-Baptista, G., Yamane, T., Oliveira, V., Juliano, L., Lapa, A.J., Lima-Landman, M.T., Hayashi, M.A., 2012. Kinetic characterization of gyroxin, a serine protease from *Crotalus durissus terrificus* venom. Biochimie 94, 2791–2793.

Yonamine, C.M., Prieto-da-Silva, A.R.B., Magalhães, G.S., Rádis-Baptista, G., Morganti, L., Ambiel, F.C., Chura-Chambi, R.M., Yamane, T., Camillo, M.A.P., 2009. Cloning of serine protease cDNAs from *Crotalus durissus terrificus* venom gland and expression of a functional Gyroxin homologue in COS-7 cells. Toxicon 54, 110–120.